The Plant Cell, Vol. 19: 1682–1694, May 2007, www.plantcell.org

Physical Association of the NB-LRR Resistance Protein Rx with a Ran GTPase–Activating Protein Is Required for Extreme Resistance to *Potato virus X* [W] [OA]

Wladimir I.L. Tameling[1] and David C. Baulcombe[2]

Sainsbury Laboratory, John Innes Centre, Norwich NR4 7UH, United Kingdom

Nucleotide binding leucine-rich repeat (NB-LRR) proteins play an important role in plant and mammalian innate immunity. In plants, these resistance proteins recognize specific pathogen-derived effector proteins. Recognition subsequently triggers a rapid and efficient defense response often associated with the hypersensitive response and other poorly understood processes that suppress the pathogen. To investigate mechanisms associated with the activation of disease resistance responses, we investigated proteins binding to the potato (*Solanum tuberosum*) NB-LRR protein Rx that confers extreme resistance to *Potato virus X* (PVX) in potato and *Nicotiana benthamiana*. By affinity purification experiments, we identified an endogenous *N. benthamiana* Ran GTPase–Activating Protein2 (RanGAP2) as an Rx-associated protein in vivo. Further characterization confirmed the specificity of this interaction and showed that the association occurs through their N-terminal domains. By specific virus-induced gene silencing of *RanGAP2* in *N. benthamiana* carrying *Rx*, we demonstrated that this interaction is required for extreme resistance to PVX and suggest that RanGAP2 is part of the Rx signaling complex. These results implicate RanGAP-mediated cellular mechanisms, including nucleocytoplasmic trafficking, in the activation of disease resistance.

INTRODUCTION

Plant disease resistance is mediated by a multilayered innate immune system that shares features with animal innate immunity (Nurnberger et al., 2004). One of these layers, referred to as pathogen-associated molecular pattern (PAMP)–triggered immunity (PTI), involves the recognition of PAMPs that are conserved microbial factors and subsequent induction of basal defenses (Zipfel and Felix, 2005; Jones and Dangl, 2006). A second layer of defense involves molecular recognition of virulence effectors of the pathogen that might have evolved to suppress PTI. A class of nucleotide binding leucine-rich repeat (NB-LRR) resistance (R) proteins has been implicated in this layer of resistance, which is referred to as effector-triggered immunity (ETI) (Jones and Dangl, 2006). This type of immunity is also known as pathogen race–host plant cultivar–specific disease resistance. ETI seems to be an accelerated and amplified PTI response (Jones and Dangl, 2006) and is often associated with a form of programmed cell death referred to as the hypersensitive response (HR) (Lam et al., 2001).

PTI and ETI have features in common with mammalian innate immunity, but they are likely to have evolved independently (Ausubel, 2005). Interestingly NB-LRR proteins, belonging to the signal transduction ATPases with numerous domains (STAND) class of P-loop NTPases (Leipe et al., 2004), are involved in both types of pathway. The C-terminal LRR domain of these proteins is largely implicated in the recognition of nonself molecules, which in plants may be mediated either by direct or indirect sensing of pathogen effectors (Deyoung and Innes, 2006). The NB domain in R proteins is proposed to act as a nucleotide-dependent molecular switch that regulates the conformation, and thereby the signaling potential, of these proteins (Takken et al., 2006). This hypothesis is largely based on studies of the nucleotide binding and intramolecular interactions with NB-LRR proteins (Moffett et al., 2002; Tameling et al., 2002, 2006). In plants, the N terminus of NB-LRR proteins is similar to a domain of Toll and Interleukin-1 receptors (TIR) or has a predicted propensity to form coiled-coil (CC) structures (Pan et al., 2000). Analysis of R protein deletion mutants suggests that these domains might be directly involved in the initiation of defense signaling (Bendahmane et al., 2002; Zhang et al., 2004), and the correlation between the N-terminal domain and the requirement of different downstream signaling factors (either EDS1 or NDR1) (Feys and Parker, 2000) is also consistent with this idea.

We are using the potato (*Solanum tuberosum*) NB-LRR protein Rx as a model for the investigation of ETI. Rx confers resistance to *Potato virus X* (PVX) by recognition of the viral coat protein (CP) (Bendahmane et al., 1995, 1999). Rx-mediated resistance is referred to as extreme resistance (Kohm et al., 1993; Bendahmane et al., 1999) because it is induced early in the viral infection cycle and involves the suppression of virus accumulation without an

[1] Current address: Laboratory of Phytopathology, Wageningen University, Binnenhaven 5, 6709 PD Wageningen, The Netherlands.
[2] To whom correspondence should be addressed. E-mail david.baulcombe@tsl.ac.uk; fax 44-1603-450011.
The author responsible for distribution of materials integral to the findings presented in this article in accordance with the policy described in the Instructions for Authors (www.plantcell.org) is: David C. Baulcombe (david.baulcombe@tsl.ac.uk).
[W] Online version contains Web-only data.
[OA] Open Access articles can be viewed online without a subscription.
www.plantcell.org/cgi/doi/10.1105/tpc.107.050880

HR. However, in experimental conditions, such as when the CP is overexpressed, there is an Rx-dependent HR, and in a previous report from this laboratory it was proposed that Rx operates similarly to other NB-LRR proteins that trigger the HR (Bendahmane et al., 1999). Consistent with that idea, Rx function requires Hsp90 and SGT1 proteins, which are also required for the functionality of other NB-LRR proteins (Peart et al., 2002b; Lu et al., 2003; Azevedo et al., 2006).

Here, we describe a targeted proteomics approach to the analysis of the molecular mechanism of Rx function in which we aimed to identify components of the Rx signaling complex. By affinity purification and mass spectrometry, we identified the endogenous *Nicotiana benthamiana* homolog of *Arabidopsis thaliana* Ran GTPase–Activating Protein2 (At RANGAP2), hereafter referred to as RanGAP2, as a specific Rx-associated protein. RanGAP proteins are highly conserved in eukaryotes and play an important role in the regulation of the activity of the small GTPase Ran (for Ras-related nuclear protein) that is essential for the nucleocytoplasmic trafficking of macromolecules through the nuclear pores (Meier, 2007). We show that reduced levels of RanGAP2 result in suppressed Rx-mediated resistance without influencing responses associated with other NB-LRR proteins. These findings implicate nucleocytoplasmic protein trafficking in the activation of Rx-mediated disease resistance.

RESULTS

Identification of Endogenous RanGAP2 as an Rx-Associated Protein

To investigate proteins in an Rx complex, we fused full-length Rx and the CC and LRR domains of Rx (amino acids 1 to 144 and 473 to 937, respectively) to a tandem affinity purification tag comprising the calmodulin and streptavidin binding peptides (csBP) (Figure 1A). Our aim was to purify the full-length Rx protein and the Rx protein fragments and to identify any associated proteins. Other Rx constructs used in our experiments included the NB-LRR (amino acids 139 to 937) and CC-NB (amino acids 1 to 477) constructs described previously (Figure 1A) (Moffett et al., 2002; Rairdan and Moffett, 2006). Expression of the fusion proteins for purification was performed by infiltration of *Agrobacterium tumefaciens* cultures into *N. benthamiana*. The expression constructs were in *Agrobacterium* T-DNA vectors under the control of the cauliflower mosaic virus (CaMV) 35S promoter.

First, we confirmed that the tagged Rx proteins were functional by transient coexpression in *N. benthamiana* leaves with the PVX CP or by stable transgenic expression. In the transient assay, the PVX CP induced an HR with the full-length tagged Rx construct, as well as upon coexpression of the tagged Rx fragments CC with the NB-LRR and LRR with the CC-NB, whereas β-glucuronidase (GUS) did not (see Supplemental Figure 1A online). In each instance, the HR intensity and timing were as with full-length Rx fused to the hemagglutinin (HA) tag (Bendahmane et al., 2002). These results are in agreement with a previous report in which it was shown that separate Rx fragments could complement Rx function in trans (Moffett et al., 2002). Transgenic *N. benthamiana* plants expressing Rx-csBP (controlled by Rx regulatory sequences) from a single T-DNA integration locus conferred extreme resistance to PVX (see Supplemental Figure 1B online). By transient coexpression of the tagged Rx fragments in *N. benthamiana* and subsequent immunoprecipitation assays, we confirmed that the Rx intramolecular interactions (Moffett et al., 2002) were not disturbed by the csBP tag (see Supplemental Figure 1C online).

We started purification of the tagged Rx-CC and Rx-LRR proteins by capture with a streptavidin matrix and elution with D-biotin. The eluted fractions contained proteins migrating as predicted for the respective tagged proteins. Both fractions also contained a protein of 55 kD that was subsequently identified as ribulose-1,5-bisphosphate carboxylase/oxygenase, but otherwise the profiles were different (Figure 1B). We then analyzed individual proteins eluted from the streptavidin matrix. These proteins were subjected to in-gel trypsin digestion and mass spectrometry, and the mass data were compared with entries in SwissProt/TrEMBL and a custom Solanaceae database. From these results, we confirmed that the Rx-LRR-csBP fraction contained two proteins corresponding to the LRR fragment of Rx and to an HSP60 (Figure 1B; see Supplemental Figure 2A online). These proteins could not be fully separated with our methods, and we have not yet investigated the functional significance of a possible LRR–HSP60 interaction.

The purified Rx-CC-csBP fraction contained an abundant protein with peptide hits matching the CC domain of Rx (Figure 1B; see Supplemental Figure 2B online), as expected. A second protein that reproducibly copurified with Rx-CC-csBP in seven independent experiments yielded peptide fragments matching a predicted protein from *N. benthamiana* corresponding to the partial EST SAL_AGN012xj08f1 (see Supplemental Figure 2C online). Based on comparison with other protein databases, we conclude that this Rx-CC–interacting protein is a *N. benthamiana* RanGAP protein. *N. benthamiana* encodes a second RanGAP (based on the partial EST SAL_UKX120xg13f1), but none of the peptides in our mass spectrometry data matched this EST.

To further analyze a possible CC–RanGAP interaction, we used rapid amplification of cDNA ends PCR to isolate full-length cDNAs corresponding to the two RanGAP homologs in *N. benthamiana*. The derived protein sequences have a domain structure identical to the two *Arabidopsis* RanGAPs (At RANGAP1 and At RANGAP2), with an N-terminal WPP domain (named after its conserved Trp-Pro-Pro motif), a central LRR domain, and a C-terminal acidic tail (Figure 1C) (Rose and Meier, 2001). Protein similarity analysis indicates that the SAL_AGN012xj08f1 and SAL_UKX120xg13f1 EST sequences correspond to the At RANGAP2 and At RANGAP1 homologs of *N. benthamiana*; thus, they are named RanGAP2 and RanGAP1 (see Supplemental Figure 3 online). Reanalysis of the mass spectrometry data with the full-length cDNA sequences revealed peptides matching all domains of RanGAP2 (Figure 1C; see Supplemental Figure 2C online), but again, no matches to RanGAP1. From these data, we infer a specific interaction of Rx-CC with RanGAP2. These two interacting proteins were similarly abundant in the eluted fraction, and we conclude that all or most of the expressed Rx-CC domain is in a complex with RanGAP2. The absence of other proteins that are as abundant as RanGAP2 in this eluted fraction (Figure 1B) indicates that this interaction is direct.

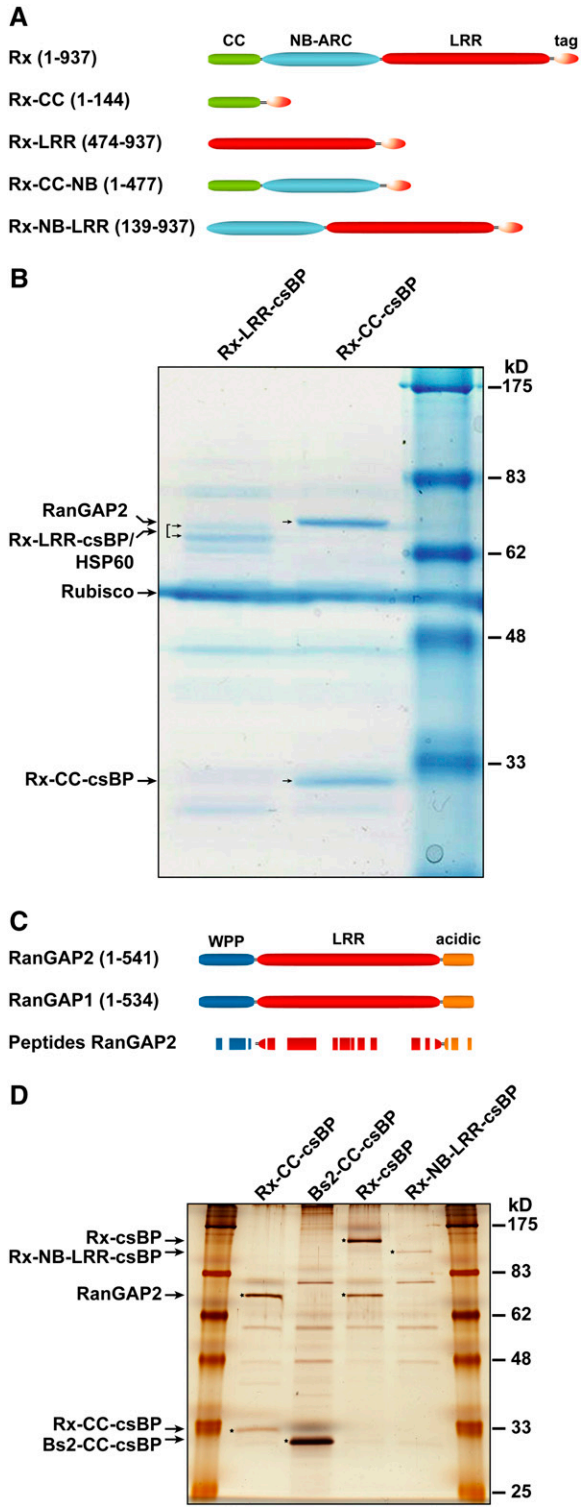

Figure 1. Copurification of Endogenous *N. benthamiana* RanGAP2 with Rx-CC-csBP.

(A) Cartoon of full-length Rx and Rx fragments fused to a csBP or Myc tag.
(B) Concentrated elution fractions of Rx-LRR-csBP and Rx-CC-csBP purifications on an SDS-PAGE gel stained with Colloidal Coomassie. The indicated protein bands were cut from the gel for mass spectrometry analysis. The identified proteins are labeled as corresponding to ribulose-1,5-bisphosphate carboxylase/oxygenase (Rubisco), Rx-CC-csBP, RanGAP2, Rx-LRR-csBP, and Hsp60 (the last two proteins could not be fully separated with our methods). The experiment was repeated three times with similar results. The Rubisco band was a contaminant from the total leaf extracts in the neighboring lanes (data not shown).
(C) Top, cartoon of domain organization in RanGAP2 and RanGAP1. Bottom, location of identified peptides from mass spectrometry analysis in the RanGAP2 sequence.
(D) Affinity-purified Rx-CC-csBP, Bs2-CC-csBP, Rx-csBP, and Rx-NB-LRR-csBP were analyzed with SDS-PAGE and silver staining. Fusion proteins and copurified endogenous RanGAP2 are indicated with arrows at left. The tagged proteins were expressed under the control of the CaMV 35S promoter in *Agrobacterium*-infiltrated *N. benthamiana* leaves that were used for the purifications in **(B)** and **(D)**.

The Rx-CC Domain Interacts with the RanGAP2-WPP Domain

Previous analyses indicated that the Rx-CC domain participates in intramolecular interactions (Moffett et al., 2002). To determine whether these interactions influence the binding of Rx-CC to RanGAP2, we analyzed full-length and deletion constructs of Rx. These tests revealed that RanGAP2 copurified with full-length Rx but not with the Rx-NB-LRR fragment (Figure 1D). We next investigated the specificity of the RanGAP interaction using the CC domain of Bs2 from pepper (*Capsicum annuum*) (amino acids 1 to 154), as Bs2 is also functional in *N. benthamiana* (Tai et al., 1999; Moffett et al., 2002; Leister et al., 2005). Bs2 is a close homolog of Rx, and their CC domains share 25% identity (see Supplemental Figure 4 online). However, RanGAP2 did not copurify with Bs2-CC-csBP, even though this tagged protein fragment was expressed abundantly (Figure 1D). The simplest conclusion of these data is that RanGAP interaction is specific to Rx and close homologs (see Discussion). However, it remains possible that secondary structural features of NB-LRR proteins or regions outside the CC domain might influence a RanGAP2 interaction. In such a situation, RanGAP interactions might be a more general feature of R protein complexes.

Further characterization with RanGAP2 constructs fused to HA epitope tags and Rx constructs fused to myc epitope tags (Figure 1A) in coimmunoprecipitation experiments (Figure 2A) confirmed the predicted interaction of RanGAP2 with Rx-CC, Rx-CC-NB, and full-length Rx. These tests also confirmed the absence of an interaction with Rx-NB-LRR and Rx-LRR fragments that lack the CC domain (Figure 2A). To determine which RanGAP2 domain is involved in the interaction with Rx, we performed coimmunoprecipitation experiments with a RanGAP2 construct that lacked the N-terminal WPP domain (RanGAP2-ΔN-HA; amino acids 107 to 541) and with RanGAP2-ΔC-HA (amino acids 1 to 112), which consists of the WPP domain only. These tests showed that the N-terminal WPP domain of RanGAP2 is involved in the association with Rx, because there was an interaction with RanGAP2-ΔC-HA but not with RanGAP2-ΔN-HA (Figures 2A and 2B). There was also no interaction with RanGAP1 fused to an HA epitope tag (Figure 2C). RanGAP1 shares 53% identity with RanGAP2 in the WPP domains (see Supplemental Figure 5 online). We conclude, therefore, that

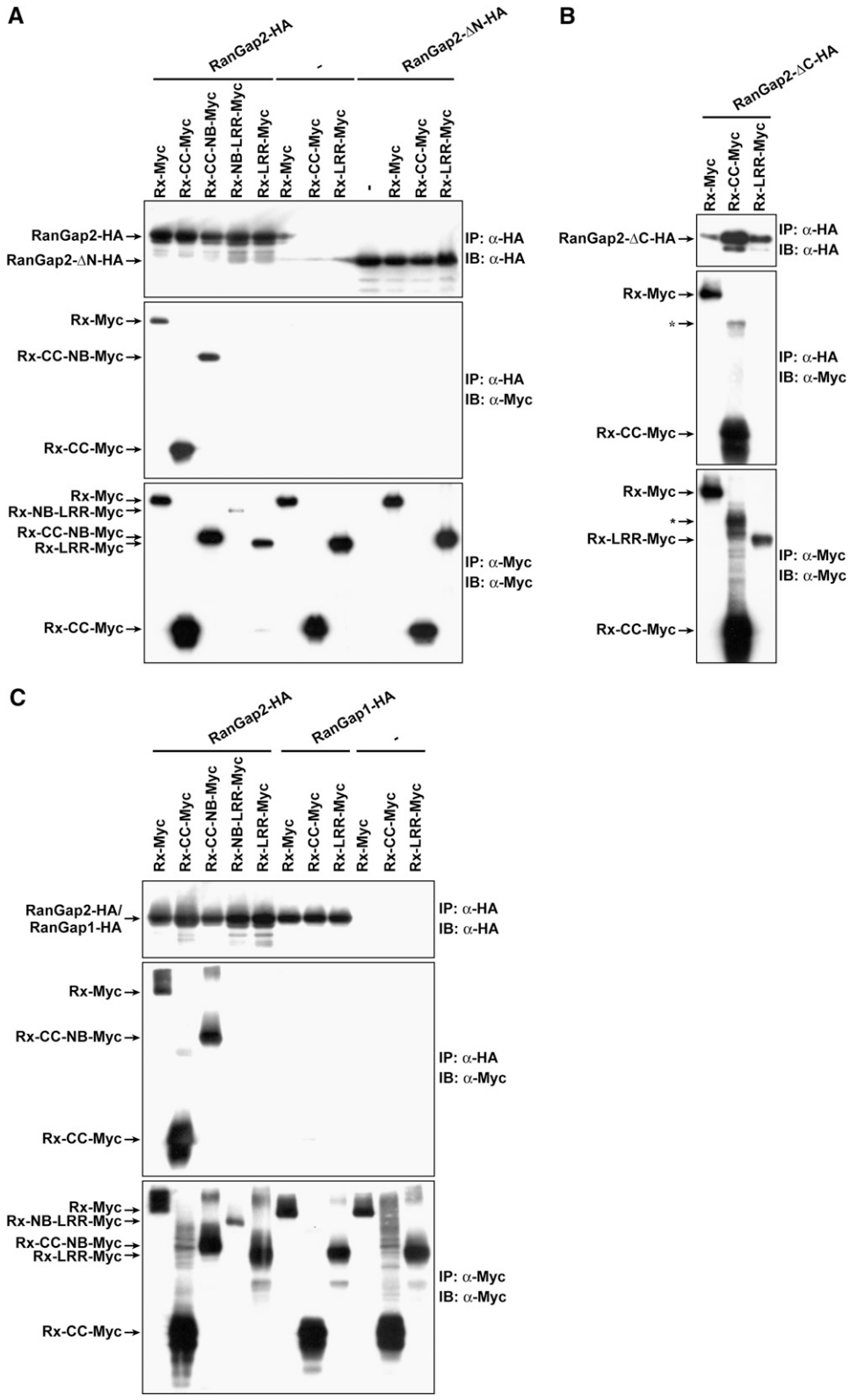

Figure 2. The WPP Domain of RanGAP2 Interacts with the CC Domain of Rx.

The indicated HA and Myc tag fusion proteins were transiently coexpressed in *N. benthamiana*, and protein extracts were subjected to coimmunoprecipitation (IP) either with anti-HA (α-HA) or anti-Myc (α-Myc) antibody. Immunoblots (IB) were analyzed with the indicated antibodies. Nonspecific signals on the blots are indicated with asterisks.

there is a specific interaction between the CC domain of Rx and the WPP domain of RanGAP2.

Silencing of *RanGAP2* Breaks Rx-Mediated Extreme Resistance to PVX

To investigate the RanGAP2 requirement for Rx-mediated extreme resistance to PVX, we used virus-induced gene silencing (VIGS) (Ratcliff et al., 2001; Liu et al., 2002) in *N. benthamiana* plants carrying Rx. Virus vector constructs based on *Tobacco rattle virus* (TRV) were inoculated to *N. benthamiana:Rx4HA* plants and an upper leaf was challenge-inoculated with PVX after 4 weeks. The initial constructs were TRV:RnGp2 (see Supplemental Figure 6A online) to silence *RanGAP2*, TRV:SGT as a positive control that would silence the *SGT1* gene that is required for Rx-mediated resistance (Peart et al., 2002b), and an empty vector, TRV:00, as a negative control.

In TRV:00-inoculated plants, the Rx-mediated resistance prevented PVX accumulation and the associated symptoms. The PVX-inoculated plants remained symptom-free for 8 weeks until the experiment was stopped (Figures 3A and 3B), and RNA gel blotting failed to detect a significant level of PVX RNA in the inoculated leaves at 6 and 8 d after inoculation (DAI) (Figure 3C). Conversely, in the TRV:SGT-inoculated plants, there was abundant accumulation of PVX RNA (Figure 3C) in the inoculated leaves, as described previously (Peart et al., 2002b), indicating that Rx-mediated resistance was lost. In TRV:RnGp2-inoculated plants, there was incomplete loss of Rx-mediated resistance manifested as necrotic lesions (Rx-induced HR), which was not observed in TRV:00- or TRV:SGT-inoculated plants. We refer to this incomplete loss of Rx-mediated resistance as loss of Rx-mediated extreme resistance. The lesions in these plants first appeared in the PVX-inoculated leaves at 7 DAI and continued to expand (Figure 3A). In the upper noninoculated leaves, the expanding systemic PVX-induced lesions started to appear at 15 DAI (Figure 3B). Correspondingly, there was a low level of PVX RNA in the inoculated leaves at 6 and 8 DAI and in the systemically infected leaves harvested at 49 DAI (Figure 3C). The necrotic lesion phenotype was reproducible in nine independent experiments involving 50 TRV:RnGp2 plants in total. The local necrotic lesions were present in 96% of the TRV:RnGp2 plants and the systemic lesions in 38%. None of the 36 TRV:00 plants exhibited necrotic lesions. The necrotic lesions in TRV:RnGp2 plants were only visible after PVX inoculation and never appeared spontaneously or after infiltration of *Agrobacterium* cultures with control, non-PVX constructs (data not shown).

It is likely that the loss of the Rx-mediated extreme resistance phenotype was due to the silencing of *RanGAP2*, because the *RanGAP2* RNA was substantially less abundant in the TRV:RnGp2 plants than in the TRV:00- and TRV:SGT-inoculated plants (Figure 3D). The probe used for this RNA gel blot analysis was designed to be specific for *RanGAP2* rather than for *RanGAP1* RNA, and its specificity was subsequently confirmed by RT-PCR (Figure 3E). In additional controls, we ruled out the possibility that the loss of Rx-mediated extreme resistance was due to an off-target effect of TRV:RnGp2 through the demonstration that TRV constructs targeted at other regions of *RanGAP2* had a similar phenotype. Thus, there was specific silencing of *RanGAP2* and PVX-induced local and systemic necrotic lesions in *N. benthamiana:Rx4HA* inoculated with TRV:RnGp2 (5′-L) or TRV:RnGp2 (5′-S) but not in plants inoculated with TRV:RnGp1 (5′-S) or TRV:GUS (see Supplemental Figures 6A to 6C online), which was used as an additional negative control.

We could also rule out the notion that the loss of Rx-mediated extreme resistance was related to an effect of *RanGAP2* silencing on the PVX-inoculation method, in which *Agrobacterium* was used as a vector system for delivery of the viral cDNA. The same loss of Rx-mediated extreme resistance was evident irrespective of whether *Agrobacterium* was used in the inoculation method. For example, when PVX was inoculated by graft inoculation, as shown in Figure 3F and Supplemental Figures 6D and 7 online, the *N. benthamiana:Rx4HA* scions developed necrotic lesions from 22 d after grafting if they had been previously infected with TRV:RnGp2 (Figure 3F), TRV:RnGp2 (5′-L), or TRV:RnGp2 (5′-S) (see Supplemental Figure 6D online) but not with TRV:00 (Figure 3F) or TRV:GUS (see Supplemental Figure 6D online).

RanGAP2 Is Required Specifically for Rx-Mediated Extreme Resistance

In principle, the loss of Rx-mediated extreme resistance in *RanGAP2*-silenced plants could result from the loss of a layer of basal PVX resistance that would otherwise limit the accumulation of the virus in plants, irrespective of whether they carry Rx. Loss of such resistance might override Rx-mediated extreme resistance. However, we were able to rule out this possibility because PVX RNA accumulation and symptoms in *N. benthamiana* without Rx were unaffected by silencing of *RanGAP2* with TRV:RnGp2 (Figures 4A to 4C).

It was also possible, in principle, that RanGAP2 could be a general cofactor of NB-LRR protein resistance mechanisms; to test this possibility, we investigated the effect of *RanGAP2* silencing on N-mediated resistance to *Tobacco mosaic virus* (TMV) and Pto/Prf-mediated resistance to *Pseudomonas syringae* pv *tabaci* (AvrPto). *N* is a TIR-NB-LRR gene that derives from tobacco (*Nicotiana tabacum*) (Whitham et al., 1994), and *Pto* is a kinase from tomato (*Solanum lycopersicum*) that requires the *CC-NB-LRR* gene *Prf* (Martin et al., 1993; Salmeron et al., 1996). Both *N* and *Pto* are functional in *N. benthamiana* (Peart et al., 2002a, 2002b). For our experiments, we used a *N. benthamiana* line that carries both *N* and *Pto* as transgenes (Peart et al., 2002b). To study the effect of *RanGAP2* silencing on Pto/Prf-mediated resistance, these transgenic plants were inoculated with TRV:RnGp2, TRV:GUS, or TRV:SGT, and after 4 weeks one leaf was challenge-inoculated with *P. syringae* pv *tabaci* (AvrPto). Resistance was broken down in TRV:SGT plants, so that significantly higher amounts of bacteria were present at days 2 and 3 than in plants infected with the negative control (TRV:GUS) (Figure 5A), as reported previously (Peart et al., 2002b). However, the amounts of bacteria found in TRV:RnGp2 plants did not differ from those in TRV:GUS plants, and we conclude that Pto/Prf-mediated resistance does not require RanGAP2. Similarly, the N-mediated resistance against TMV was not affected by silencing of *RanGAP2*, as TMV-GFP (for green fluorescent protein) RNA accumulation was the same irrespective of whether

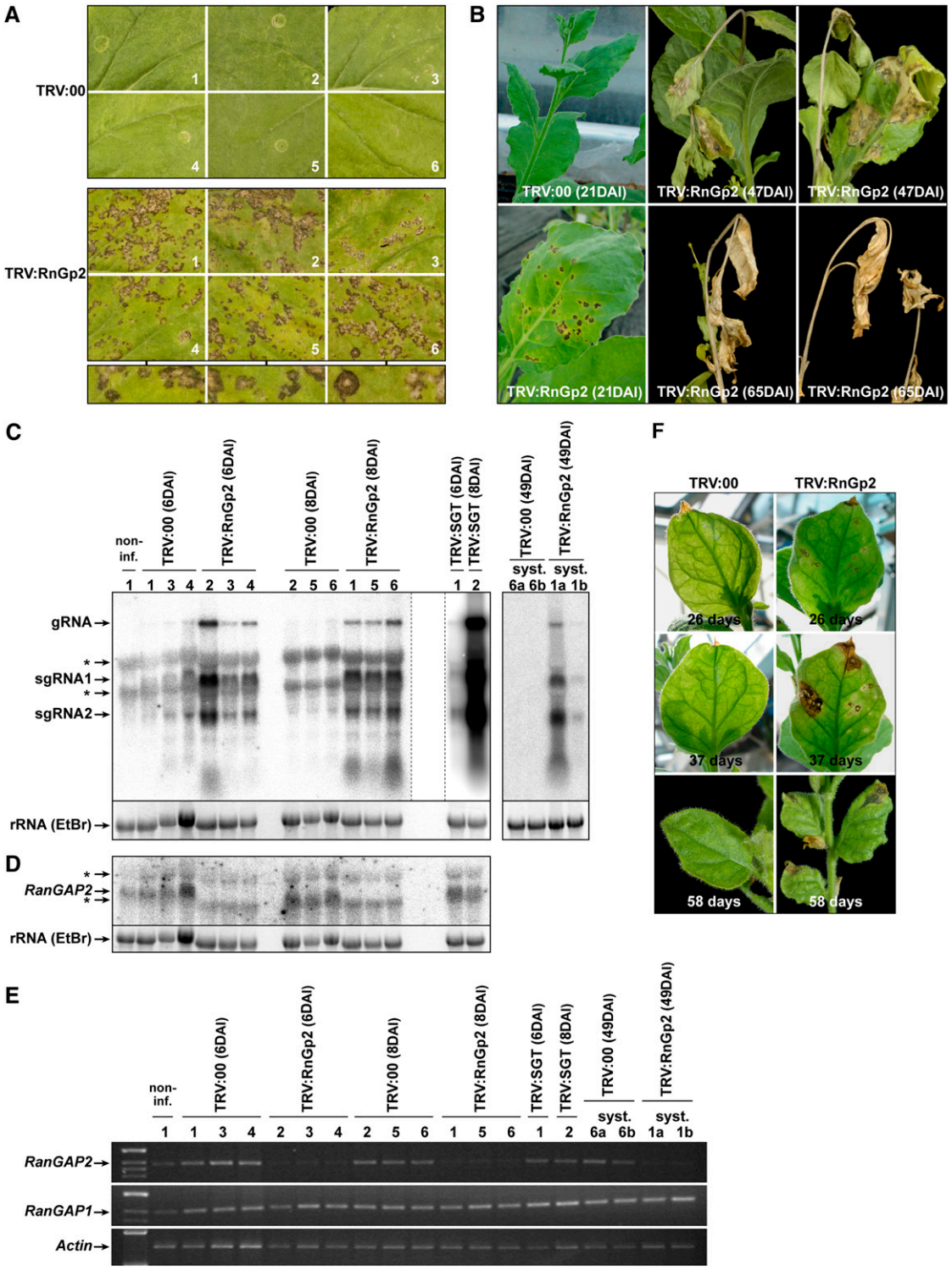

Figure 3. Silencing of *RanGAP2* Breaks Rx-Mediated Extreme Resistance.

PVX-resistant *N. benthamiana:Rx4HA* plants were inoculated with TRV:00 (empty vector), TRV:RnGp2, or TRV:SGT. Four weeks after inoculation, one leaf per plant was challenge-inoculated with PVX. Local and systemic necrotic lesions appeared only in TRV:RnGp2 plants.

(A) Top, local PVX-inoculated leaves of different plants were photographed at 16 DAI with PVX. Bottom, blowup of lesions in TRV:RnGp2 plants 4, 5, and 6. Numbers indicate individual plants and correlate to numbers in **(C)** to **(E)**.

the plants were previously infected with TRV:RnGp2 or TRV:00, whereas, as reported previously (Peart et al., 2002b), silencing of *SGT1* with TRV:SGT compromised the ability of N to limit TMV-GFP RNA accumulation (see Supplemental Figures 8A and 8B online) and the development of GFP foci (data not shown). From these data, we conclude that specific downregulation of *RanGAP2* affects Rx-mediated extreme resistance specifically rather than R protein–mediated resistance in general.

DISCUSSION

Loss of Rx-Mediated Extreme Resistance Associated with *RanGAP2* Silencing

Here, we describe a physical association in *N. benthamiana* between RanGAP2 and the NB-LRR protein Rx that confers extreme resistance against PVX (Figures 1 and 2). RanGAP proteins are structurally and functionally highly conserved in eukaryotes and play an important role in the regulation of the small GTPase Ran, which is essential for nucleocytoplasmic trafficking of macromolecules through the nuclear pores. At the cytoplasmic side of the nuclear pores, RanGAP stimulates the GTPase activity of Ran and thereby the release of Ran from import or export receptors (Merkle, 2001; Meier, 2007). Silencing of *RanGAP2* in *N. benthamiana* carrying Rx enhanced PVX-induced symptoms and PVX-derived RNA accumulation (Figures 3A to 3C; see Supplemental Figures 6B, 6D, and 7A online), and we infer that the Rx–RanGAP2 interaction is required for either the recognition or activation steps of Rx-mediated extreme resistance. However, the PVX-induced necrotic symptoms associated with *RanGAP2* silencing on Rx genotype plants were unlike the mild mosaic associated with full susceptibility to this virus and are similar to the spreading HR associated with partial loss-of-function *R* gene mutants (Dinesh-Kumar et al., 2000). Presumably, the spreading HR occurs when the pathogen effector is recognized weakly or when the downstream signaling is inefficient. In this scenario, the resistance mechanism would be activated too slowly to prevent spread of the pathogen.

Consistent with this interpretation, the accumulation of PVX RNA in the *RanGAP2*-silenced Rx genotype plants was substantially higher than in the unsilenced Rx control but much less than in fully susceptible wild-type plants or plants silenced for the Rx cofactor *SGT1* (Figures 3C and 4A; see Supplemental Figure 7A online). To explain the partial loss of Rx resistance against PVX, we propose that there is residual RanGAP2 protein in the silenced plants that is sufficient to support a reduced level of resistance. We also considered the possibility that RanGAP1 can interact with Rx in the absence but not in the presence of RanGAP2. However, a RanGAP1 interaction is not likely, since Rx-CC-csBP did not interact with RanGAP1-HA in wild-type plants inoculated with TRV:RnGp2 and in which the levels of RanGAP2 were reduced (see Supplemental Figure 9A online).

In independent research, potato RanGAP2 associated not only with Rx but also with the close Rx homologs Rx2 and Gpa2 (Sacco et al., 2007). The Rx2-CC domain is almost identical to that of Rx (Bendahmane et al., 2000); therefore, it is expected that the interaction with potato RanGAP2 would also be required for Rx2-mediated resistance to PVX. Gpa2 also has a CC domain that is almost identical to that of Rx, but whether this RanGAP2 interaction is also required for Gpa2-mediated resistance to the potato cyst nematode *Globodera pallida* (van der Vossen et al., 2000) is an intriguing question to be answered in the future.

It is striking that the *RanGAP2*-silencing phenotype is specific for Rx and not for the NB-LRR resistance proteins N and Pto/Prf (Figure 5; see Supplemental Figures 8A and 8B online). This phenotypic specificity is consistent with the high specificity of the RanGAP2–Rx-CC interaction, as indicated by its failure to bind the N-terminal domain of NB-LRR protein Bs2 from pepper (Figure 1D). The phenotype specificity also has clear implications for our interpretation of the role of RanGAP2 in disease resistance. Most significantly, it is evidence against the loss of resistance being a pleiotropic consequence of disrupted nucleocytoplasmic trafficking. In that situation, the Pto/Prf- and N-mediated resistance mechanisms would have also been compromised in the *RanGAP2*-silenced plants, because these resistance mechanisms have other molecular features in common with Rx-mediated resistance. The absence of a disrupted growth

Figure 3. (continued).

(B) Systemically infected leaves of representative TRV:00 and TRV:RnGp2 plants were photographed at the indicated time points after PVX inoculation.

(C) Lesion formation correlates with higher accumulation of PVX RNAs. Top, RNA gel blot analysis with a PVX CP probe. Local leaves were harvested at 6 and 8 DAI, and systemic (syst.) leaves were harvested at 49 DAI for RNA extraction. Tissue of a noninfected plant (non-inf.; no TRV/PVX inoculation) of the same age was used as a control. PVX genomic (g) RNA and subgenomic (sg) RNA1 and sgRNA2 are indicated as well as nonspecific signal of the CP probe to rRNAs (asterisks). Ethidium bromide (EtBr)–stained rRNA was used as a loading control. The lanes of the TRV:SGT samples were cut off the membrane and used for a separate exposure. The intensity of the signal was adjusted to visualize the separate bands; therefore, the signal intensity of these lanes cannot be compared with the additional lanes. The signal was at least 2 orders of magnitude higher than in TRV:RnGp2 lanes.

(D) RanGAP2 transcript was reduced in abundance in TRV:RnGp2 plants. Samples, layout, and procedures were as in **(C)**, except that the blot was hybridized with a RanGAP2-specific probe.

(E) RT-PCR analysis indicates specific silencing of *RanGAP2*. RT-PCR was performed with primers designed to specifically detect *RanGAP2*, *RanGAP1*, and *Actin* transcripts.

(F) Young PVX-resistant *N. benthamiana:Rx4HA* plants were inoculated with TRV:00 (empty vector) or TRV:RnGp2. Four weeks later, the apex of the plants were grafted on top of root stocks derived from wild-type susceptible *N. benthamiana* plants systemically infected with PVX. Necrotic lesions were observed only in scion leaves derived from TRV:RnGp2 plants. Photographs were taken at the indicated time points (indicating days after grafting).

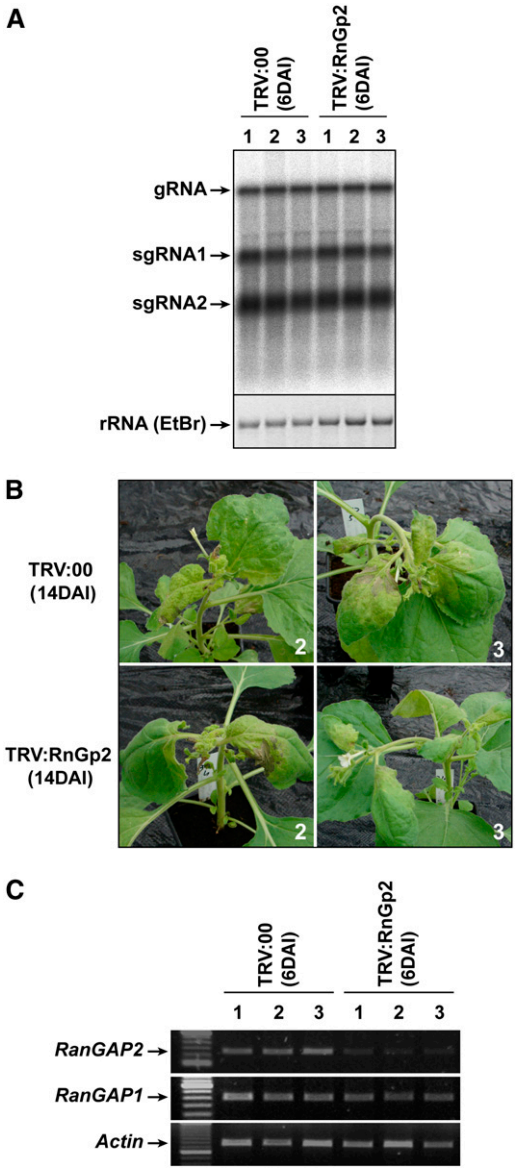

Figure 4. Silencing of *RanGAP2* Does Not Affect PVX Replication and Movement in Susceptible Plants.

PVX-susceptible *N. benthamiana* plants, lacking Rx, were inoculated with TRV:00 and TRV:RnGp2, and 4 weeks later one leaf per plant was challenge-inoculated with PVX.

(A) No difference in the accumulation of PVX RNAs in PVX-infiltrated leaves. PVX-infiltrated leaves were harvested at 6 DAI, and extracted RNA was analyzed by RNA gel blotting with the CP probe. For an explanation of figure layout and abbreviations, see legend to Figure 3C.

(B) No difference in disease (mosaic) symptoms in systemic tissue. Two representative TRV:00 and TRV:RnGp2 plants were photographed at 14 DAI.

(C) RT-PCR analysis indicates specific silencing of *RanGAP2*. Numbers indicate individual plants and correlate between all panels.

phenotype is also evidence against the possibility of pleiotropic effects in *RanGAP2*-silenced *N. benthamiana* (data not shown).

Rx Interaction with RanGAP2 and the Guard Hypothesis

To explain the role of RanGAP2 in Rx-mediated resistance mechanisms, we offer two alternative hypotheses. The first of these is based on the guard hypothesis of disease resistance (Jones and Dangl, 2006) and requires that RanGAP2 is a virulence target of the PVX effector protein CP. According to this hypothesis, the biochemical or cellular properties of RanGAP2 are influenced either by direct binding to the PVX CP or through indirect effects of the CP. The interaction of Rx with RanGAP2 would thus allow the NB-LRR protein to be a sensor for the perturbations of RanGAP2 by the effector molecule. In this scenario, Rx would guard RanGAP2 and the effect of the CP would explain the initiation of Rx-mediated ETI, resulting in extreme resistance to PVX. A similar guard mechanism has been proposed for the *Arabidopsis* NB-LRR protein HRT that triggers ETI upon recognition of turnip crinkle virus CP. The CP binds and thereby blocks the translocation of a putative transcription factor into the nucleus (Ren et al., 2005).

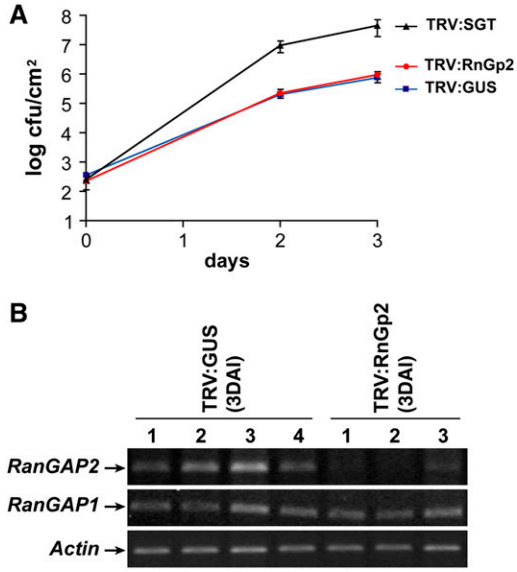

Figure 5. Silencing of *RanGAP2* Does Not Affect Pto-Mediated Resistance.

N. benthamiana plants carrying the tomato R gene *Pto* that are resistant to *P. syringae* pv *tabaci* (AvrPto) were inoculated with the indicated TRV-silencing constructs. Four weeks after inoculation, resistance to this pathogen was tested.

(A) No difference in *P. syringae* pv *tabaci* (AvrPto) growth between TRV:GUS (negative control) and TRV:RnGp2 plants. The indicated plants were infiltrated with *P. syringae* pv *tabaci* (AvrPto) in one leaf per plant. Bacterial growth in these leaves was monitored for 3 d. Each data point represents the mean ± SD of six replicate samples.

(B) RT-PCR analysis at 3 DAI with *P. syringae* pv *tabaci* (AvrPto) indicates specific silencing of *RanGAP2*.

However, an in planta interaction between RanGAP2 and PVX CP was not found in pull-down experiments (see Supplemental Figure 9B online). A further difficulty with this variation of the guard hypothesis is the implication that the interaction of RanGAP2 and Rx-CC is part of the molecular recognition mechanism of Rx-mediated resistance (Figures 1 and 2). Previous evidence implicates the LRR domain rather than the CC in the molecular recognition process (Farnham and Baulcombe, 2006). The guard mechanism is not disproved by these data, but on balance, we find a second hypothesis more attractive, one that, as discussed below, involves an effect on trafficking of proteins between the cytoplasm and the nucleus.

Rx Interaction with RanGAP2 and Nucleocytoplasmic Trafficking of Proteins

Our alternative hypothesis proposes that the interaction of Rx with RanGAP2 influences the trafficking of resistance-related proteins through the nuclear pores and implicates the Rx-CC domain in signaling rather than recognition. RanGAPs exert their activity at the cytoplasmic side of the nuclear envelope to which they are targeted in interphase cells (Meier, 2007). In plants, this targeting is mediated by the plant-specific N-terminal WPP domain (Rose and Meier, 2001). As the WPP domain is bound by Rx (Figure 2B), we envision that activation of Rx might influence RanGAP2 targeting at the nuclear envelope and, consequently, Ran GTPase activation and trafficking of proteins into the nucleus. Alternatively, the binding of Rx might also directly affect this activity without changing the subcellular localization of RanGAP2. This influence could be mediated by the conformational changes in Rx associated with its activation (Moffett et al., 2002).

There are several lines of supporting evidence to implicate nucleocytoplasmic trafficking in plant disease resistance mechanisms. For example, the *Arabidopsis mos3-1* mutant that suppresses the constitutive defense phenotype of a mutant TIR-NB-LRR protein (snc1) (Zhang et al., 2003) is a nucleoporin Nup96 loss-of-function allele (Zhang and Li, 2005). Besides a decrease in basal defense, the *mos3-1* mutation also leads to reduced R protein–mediated resistance (Zhang and Li, 2005). A second *snc1*-suppressor mutant, *mos6*, contains a mutation in an *Arabidopsis* Importin α (At Impα3) (Palma et al., 2005). Importin α proteins bind to cargo with a nuclear localization signal and mediate nuclear import through the Ran-regulated (including RanGAP) nuclear pore complex (Merkle, 2001; Meier, 2007). These findings, together with our data showing a role of RanGAP2, prompt the speculation that CP-induced Rx activation requires nucleocytoplasmic protein trafficking of disease resistance cofactors. Such cofactors could be proteins like NPR1, TGA, or bZIP transcription factors and mitogen-activated protein kinases that are implicated in disease resistance and translocate to the nucleus upon activation of the defense response (van der Krol and Chua, 1991; Ligterink et al., 1997; Cheong et al., 2003; Ahlfors et al., 2004; Dong, 2004; Lee et al., 2004; Pedley and Martin, 2005; Kaminaka et al., 2006).

Nucleocytoplasmic trafficking could also affect disease resistance if the NB-LRR proteins are nuclear. Strikingly, Rx has been detected as a nuclear protein (J. Bakker, personal communication), and there are three other reports of nucleus-localized NB-LRR proteins. The nuclear localization of the barley (*Hordeum vulgare*) CC-NB-LRR protein MLA10, for example, is required for resistance to a *Blumeria graminis* f sp *hordeii* strain carrying the cognate effector gene Avr_{A10} (Shen et al., 2007). Another example involves the atypical *Arabidopsis* TIR-NB-LRR protein RRS1-R, which also has a WRKY transcription factor domain. RRS1-R is located in the nucleus, but only when the interacting cognate effector protein is coexpressed (Deslandes et al., 2003). In the third example, the elicitation of N-mediated resistance responses by the p50 effector protein of TMV requires the nuclear localization of N (Burch-Smith et al., 2007). Perhaps the nuclear import of Rx is specifically mediated through physical association with RanGAP2. As Rx does not contain a predicted nuclear localization signal sequence, we envisage that cofactors containing a nuclear localization signal are carriers for the R proteins (Tzfira et al., 2001) and that the interaction with RanGAP2 might mediate the loading of Rx onto such a carrier protein at the nuclear envelope. Another possibility, however, is that RanGAP2 itself functions as the Rx carrier. If nuclear localization of NB-LRR proteins is a general feature, then with NB-LRR proteins that do not interact directly with a RanGAP2, like Bs2 (Figure 1D) and presumably Prf (Figure 5) and N (see Supplemental Figures 8A and 8B online), there could still be an effect of RanGAP on their nucleocytoplasmic trafficking. It could be either that other isoforms of RanGAP are involved or that their effect is indirect and mediated via other as yet unidentified factors that interact with NB-LRR proteins.

At present, the Rx-CC interaction with a RanGAP2 is atypical. It has only been described for the NB-LRR protein Rx and its close homologs Rx2 and Gpa2, and RanGAP mutations have not been identified in loss of disease resistance screens. However, the discovery of this interaction and its influence on Rx-mediated extreme resistance to PVX, as described here, both reinforce the significance of nucleocytoplasmic protein trafficking in disease resistance. Also, the movement of resistance-related kinases, transcription factors, and Rx and other NB-LRR proteins into the nucleus illustrates how nucleocytoplasmic protein trafficking may have a general significance in the activation of ETI.

METHODS

Plant Material

Wild-type *Nicotiana benthamiana*, *N. benthamiana:Rx4HA* (Lu et al., 2003), *N. benthamiana* carrying *Rx*, *N*, and *Pto* (Peart et al., 2002b), and *N. benthamiana* containing pB1-Rx-csBP (under the control of the Rx regulatory sequences) were grown in glasshouses under controlled light and temperature. Wild-type *N. benthamiana* was transformed with the pB1-Rx-csBP construct. A line carrying a single T-DNA integration locus was brought to homozygosity (line 3108-H1) and used for the PVX resistance assay.

Plasmid Construction

pC/SBPc is a pBIN61 (Bendahmane et al., 2002) vector containing the sequence of a tandem affinity tag encoding the calmodulin binding peptide

(KRRWKKNFIAVSAANRFKKISSSGAL) and the streptavidin binding peptide (MDEKTTGWRGGHVVEGLAGELEQLRARLEHHPQGQREP) for C-terminal fusions and the CaMV 35S promoter. Full-length Rx, Rx fragments, and the Bs2-CC fragment were excised using *Xba*I and *Bam*HI from Rx-HA and Bs2-HA fusion constructs containing the CaMV 35S promoter (Moffett et al., 2002) and ligated into the *Xba*I/*Bam*HI sites of pC/SBPc, creating C-terminal in-frame fusions with the csBP tag. Rx-Myc and Rx-HA constructs are based on the pBIN61 vector containing the CaMV 35S promoter and are described by Moffett et al. (2002). To create pB1-Rx-csBP (containing Rx regulatory sequences), full-length Rx fused to the csBP tag was excised from the described CaMV 35S construct with *Xba*I and *Sac*I and used for replacement of the Rx-HA fusion in pB1-Rx-HA (Bendahmane et al., 2002).

The CP32-csBP construct (SLDB3059) encodes amino acids 32 to 142 of PVX_{CP4} and was created based on the GFP-CP32-TK construct (Moffett et al., 2002). CP32 was amplified by PCR from this construct with oligonucleotides 5′-CTAGTCTAGAATGACTATACCAGATGGGGAC-3′ and 5′-CCATCTTCTCTTCGGGCTGTTGTTTGTTAAC-3′, by which a 5′ *Xba*I site (underlined) and a 3′ sequence identical to the 5′ end of the csBP tag were introduced. The csBP tag was amplified by PCR from the pC/SBPc vector with oligonucleotides 5′-CAACAGCCCGAAGAGAAGATG-GAAGAAGAAC-3′ and 5′-GTACCCCGGGTTAAGGCTCTCTCTGTCC-TTG-3′, introducing a 5′ sequence identical to the 3′ end of the CP32 fragment and a 3′ *Sma*I site (underlined). The two PCR fragments were fused by overlap extension PCR, and the fusion was ligated into the *Xba*I/*Sma*I sites of pBIN61. The CP-SBP construct (SLDB3060) encodes the entire CP of PVX_{CP4} and was derived from the 35S-TK construct described by Bendahmane et al. (2002). CP was amplified by PCR with oligonucleotides 5′-CGGTCTAGAATGACTACACCAGCCAACAC-3′ and 5′-CTTCTCATCCATTGGTGGGGGTAGTGAAAC-3′, introducing a 5′ *Xba*I site (underlined) and a 3′ sequence identical to the 5′ end of the SBP encoding part of the csBP tag. The SBP fragment was amplified from the pC/SBPc vector with oligonucleotides 5′-CTACCCCCACCAATGG-ATGAGAAGACTACTGG-3′ and 5′-GTACCCCGGGTCAAGGCTCTCTC-TGTCCTTG-3′, introducing a 5′ sequence identical to the 3′ end of the CP fragment and a 3′ *Sma*I site (underlined). The two PCR fragments were fused by overlap extension PCR and ligated into the *Xba*I/*Sma*I sites of pBIN61.

Full-length cDNAs of *N. benthamiana RanGAP1* and *RanGAP2* were obtained using the GeneRacer kit (Invitrogen). KOD HIFI DNA polymerase (Novagen) was used for amplification of the complete *RanGAP1* coding sequences with oligonucleotides wo111 (5′-GTCGACATGGATTCTGC-AGGATTCTCTCTGA-3′) and wo112 (5′-GGATCCTTCTTCCTGCTTG-ATATCAAGACCC-3′) and of *RanGAP2* with oligonucleotides wo076 (5′-GTCGACATGGATGCCACAACGCCGAATTC-3′) and wo077 (5′-GGA-TCCCTTGACGTCAAGGTTTTTGAGTTTTG-3′). The stop codons were deleted for C-terminal HA epitope fusion, and 5′ *Sal*I and 3′ *Bam*HI sites (underlined) were added for cloning into the *Sal*I/*Bam*HI sites of pBIN61-cHA (SLDB3125). pBIN61-cHA was constructed by replacing the Rx-CC *Xba*I/*Bam*HI fragment in pBIN61-Rx-CC-HA (SLDB2502; Moffett et al., 2002) with a linker based on oligonucleotides wo004 (5′-CTAGAGTC-GACCCTCGAGTG-3′) and wo005 (5′-GATCCACTCGAGGGTCGACT-3′) to introduce a *Sal*I site (underlined). Ligation of the RanGAP fragments in this vector resulted in the constructs pBIN61-NbRanGAP2-HA (SLDB3154) and pBIN61-NbRanGAP1-HA (SLDB3182). For pBIN61-NbRanGAP2-ΔN-HA (SLDB3174), a *RanGAP2* fragment was amplified by PCR with oligonucleotides wo090 (5′-TGTCGACATGGAGGAAAAGGAGATTTC-AATCT-3′) and wo077, introducing a 5′ *Sal*I site (underlined) followed by a start codon, and a 3′ *Bam*HI site, which was subsequently cloned into the *Sal*I/*Bam*HI sites of pBIN61-cHA. For pBIN61-NbRanGAP2-ΔC-HA (SLDB3159), the same acceptor plasmid was used to clone the amplified *RanGAP2* fragment. This fragment was obtained by PCR with oligonucleotides wo076 (5′-GTCGACATGGATGCCACAACGCCGAA-TTC-3′) and wo091 (5′-GGATCCTGAAATCTCCTTTTCCTCTGTT-3′), introducing a 5′ *Sal*I site and a 3′ *Bam*HI site (underlined). The *RanGAP2* deletions in these constructs correspond to the At RANGAP1ΔN-GFP and At RANGAP1ΔC-GFP deletion constructs described by Rose and Meier (2001).

For VIGS experiments, DNA fragments of *N. benthamiana RanGAP2*, *RanGAP1*, and *GUS* (as a negative control) were inserted into the pTRV2 vector (Liu et al., 2002). For TRV:RnGp2 (SLDB3162), a *RanGAP2* fragment (587 bp) was amplified by PCR with oligonucleotides wo092 (5′-TCGAATTCGGATCCGCCTTGTGTGAAGCACTTGG-3′) and wo093 (5′-AACTCGAGTCTAGATCGTCATCTTCTCTCACTGG-3′), introducing *Xba*I and *Bam*HI sites (underlined), and cloned into the *Xba*I/*Bam*HI sites of pTRV2. For TRV:RnGp2 (5′-L) (SLDB3178), an *Xba*I fragment from SLDB3154 (635 bp) corresponding to the 5′ part of *RanGAP2* was cloned into the *Xba*I site of pTRV2. For TRV:RnGp2 (5′-S) (SLDB3176) and TRV:RnGp1 (5′-S) (SLDB3177), specific fragments were first amplified by PCR with oligonucleotides wo033 (5′-CGCAAGTACCGCAGTCTATCC-3′) and wo034 (5′-AGCAACACGTGCTGCGCCTCG-3′) (amplifying 387 bp of *RanGAP2*) and wo037 (5′-AGGAAATATGGCCTTTTAAGT-3′) and wo038 (5′-CCTGCAATTTTAGCAGCATCCAC-3′) (amplifying 395 bp of *RanGAP1*), respectively, and subsequently subcloned into the pGEM T-easy vector (Promega). The plasmids were incubated first with *Nco*I, and the site was blunt-ended using Klenow fragment. Thereafter, digestion with *Spe*I was used to excise the RanGAP fragments, which were subsequently cloned into the *Xba*I/*Sma*I sites of pTRV2. For TRV:GUS (SLDB3180), a fragment of the GUS coding sequence (636 bp) in pBIN61-GUS was amplified by PCR with oligonucleotides 5′-ACGTCCTGTAGAAACCCC-3′ and 5′-GAC-TCGAGATCACCATTGGCCACCAC-3′ and ligated into the PCR Blunt II TOPO vector. The fragment was excised with *Eco*RI and cloned into the *Eco*RI site of pTRV2.

Agroinfiltration

Binary plasmids were used in *Agrobacterium tumefaciens* strain C58C1 carrying the helper plasmid pCH32. Transient expression was performed as described by Mestre and Baulcombe (2006). Suspensions of *Agrobacterium* carrying Rx or RanGAP constructs were infiltrated at $OD_{600} = 0.3$. Coexpression was performed by mixing equal volumes of the suspensions.

Protein Purification

For the protein isolation method and immunoprecipitation assay, procedures were followed as described by Moffett et al. (2002). For purification of the transiently expressed csBP fusion proteins shown in Figures 1B and 1D, 8.0 and 2.5 g of tissue were used, respectively, and the extracts were incubated with 540 and 100 μL bed volumes of Streptavidin Sepharose High Performance (GE Healthcare). End-over-end protein capture was performed for 3 h at 4°C, and washing was done as in the immunoprecipitation assays. Elution was performed twice with 2 bed volumes of wash buffer containing 4 mM D-biotin (Sigma-Aldrich). Elution fractions were pooled and precipitated with trichloroacetic acid. The pellets were washed with 100% acetone at −20°C and resuspended in 1× SDS-PAGE loading buffer. For Figures 1B and 1D, 40 and 30 μL of 45× and 15× concentrated samples, respectively, were loaded on SDS-PAGE gels. The gels were subsequently subjected to Colloidal Coomassie or silver staining. For Colloidal Coomassie staining, the gel was immersed overnight in staining solution (0.07% [w/v] Coomassie Brilliant Blue G 250, 34% [v/v] methanol, 17% [w/v] ammonium sulfate, and 3% [v/v] phosphoric acid) and destained in water. Silver staining was performed according to Blum et al. (1987). The csBP, HA, and Myc tag proteins were detected by immunoblotting (Moffett et al., 2002) using anti-calmodulin binding protein epitope tag (Upstate), anti-HA peroxidase (clone 3F10; Roche), and c-Myc (9E10)HRP (Santa Cruz), respectively. Protein bands

on Colloidal Coomassie–stained gels were excised, reduced with DTT, alkylated with iodoacetamide, and cleaved with trypsin (Promega). Purified peptides were analyzed by tandem mass spectrometry (see below).

Mass Spectrometry

Nanoflow liquid chromatography–tandem mass spectrometry analysis was performed using a LTQ mass spectrometer (Thermo Electron) employing automated data-dependent acquisition. A nanoflow HPLC system (Surveyor; Thermo Electron) was used to deliver a flow rate of ~250 nL/min to the mass spectrometer. Chromatographic separation was accomplished using a precolumn (C18 pepmap100; LC Packings) connected to a self-packed C18 8-cm analytical column (Picotip 75 μm i.d., 15-μm tip; New Objective). Peptides were eluted by a gradient of 2 to 50% acetonitrile over 48 min. The mass spectrometer was operated in positive ion mode with a nanospray source and a capillary temperature of 200°C. No sheath gas was employed, and the source voltage and focusing voltages were optimized for the transmission of angiotensin. Data-dependent analysis consisted of the six most abundant ions in each cycle: m/z 300 to 2000, minimum signal of 1000, collision energy of 25, five repeat hits, and 300-s exclusion.

Raw data were processed using BioWorks 3.2 and TurboSEQUEST (Thermo Electron) and searched against all protein entries in the SwissProt/TrEMBL database (227,000 sequences). All data were also searched against a custom Solanaceae EST database derived from plant assembled transcripts from The Institute for Genomic Research database and supplemented with in-house EST data. RanGAP cDNA sequences were added to both databases as they were obtained. In all cases, oxidized Met was included as a variable modification, and peptide hits were filtered by Xcorr and charge state [xc (+1, 2, 3) 2.0, 2.5, 3.5] and protein hits by probability (1e-003).

VIGS and Pathogen Assays

VIGS was performed as described by Ratcliff et al. (2001). TRV:00 and TRV:SGT1 are described by Peart et al. (2002b). TRV:RnGp2, TRV:RnGp2 (5′-L), TRV:RnGp2 (5′-S), TRV:RnGp1 (5′-S), and TRV:GUS are based on vectors described by Liu et al. (2002) (see above). Four weeks after TRV inoculation, pathogen assays were performed. For the Rx resistance tests, TRV-inoculated *N. benthamiana:Rx4HA* plants were challenge-inoculated by agroinfiltration in one leaf with an *Agrobacterium* suspension ($OD_{600} = 0.005$) carrying the binary PVX plasmid pGR106 (Lu et al., 2003). The same experiment was performed with wild-type *N. benthamiana* to test replication and movement in susceptible plants. For the Rx resistance test using grafting, the apices of TRV-inoculated *N. benthamiana:Rx4HA* plants were cut and grafted onto wild-type PVX-infected rootstocks, which were cut from systemic PVX-infected plants at 7 d after agroinfiltration with pGR106 in a lower leaf. The grafting procedure was performed as described by Bendahmane et al. (1999). To test N resistance, TMV-GFP was challenge-inoculated on TRV-inoculated *N. benthamiana* plants carrying *Rx*, *N*, and *Pto* by agroinfiltration of an *Agrobacterium* suspension ($OD_{600} = 0.005$) carrying the binary TMV-GFP plasmid (Peart et al., 2002a). In independent experiments, the same plants were used for the Pto/Prf resistance tests. Infection and growth of *Pseudomonas syringae* pv *tabaci* expressing AvrPto was monitored as described by Peart et al. (2002a).

RNA Gel Blot Analysis

Total RNA was isolated using Tri reagent (Sigma-Aldrich) according to the manufacturer's instructions. RNA was separated on a 1% (w/v) agarose-formaldehyde gel, transferred to a nylon membrane (Hybond-NX), and cross-linked with UV illumination. PVX and TMV-GFP RNA were detected as described by Schwach et al. (2005) and Peart et al. (2002a), respectively.

RT-PCR

cDNA synthesis was performed with 1 μg of total RNA, hexameric random primers, and the SuperScript II reverse transcriptase kit (Invitrogen) according to the manufacturer's instructions. A negative control of each RNA sample was made by omitting reverse transcriptase in the reaction. The reactions were used for the amplification of DNA fragments within the cDNAs of *N. benthamiana RanGAP2*, *RanGAP1*, and *Actin* by PCR. *RanGAP2* was amplified using 25 cycles with the oligonucleotides wo033 and wo034, *RanGAP1* using 30 cycles with wo037 and wo038, and *Actin* using 23 cycles with NbActin-F (5′-ATGGCAGATGGAGAGGATATTC-3′) and NbActin-R (5′-CCTGCCCATCCGGTAGCTCAT-3′). *Actin* mRNA levels served as internal standards. Alternative primers used to amplify *RanGAP2* and *RanGAP1* are shown in Supplemental Figure 6C online (middle two panels). These RT-PCRs were performed with wo117 (5′-GCTCCTTCAGTCTCAAACC-3′) and wo118 (5′-TTGCTGAGTGCCTTACTTAGC-3′) and with wo123 (5′-CTTTTCTTCTGCTTTGGGTGCC-3′) and wo124 (5′-GATTGATAGTACTTTGCTCAAGG-3′) using 32 and 30 cycles, respectively.

Accession Numbers

The cDNA sequences of *N. benthamiana* RanGAP1 and RanGAP2 are deposited in the GenBank database under accession numbers EF396238 and EF396237, respectively. Arabidopsis Genome Initiative locus identifier numbers for the *Arabidopsis* RanGAPs are At3g63130 (RanGAP1) and At5g19320 (RanGAP2). Accession numbers of additional sequences can be found in Supplemental Figure 3 online.

Supplemental Data

The following materials are available in the online version of this article.

Supplemental Figure 1. Functionality Control Assays of Rx Constructs Containing the csBP Tag.

Supplemental Figure 2. Peptide Hits of the Rx-CC-csBP, Rx-LRR-csBP, and RanGAP2 Bands.

Supplemental Figure 3. Similarity Analysis of Plant RanGAP Proteins.

Supplemental Figure 4. Similarity between Rx-CC and Bs2-CC.

Supplemental Figure 5. Similarity between WPP Domains of RanGAP1 and RanGAP2.

Supplemental Figure 6. VIGS with Multiple TRV:RnGp2 Constructs Suppresses Rx-Mediated Extreme Resistance.

Supplemental Figure 7. Silencing of *RanGAP2* Breaks Extreme Resistance in Grafts.

Supplemental Figure 8. Silencing of *RanGAP2* Does Not Affect N-Mediated Resistance.

Supplemental Figure 9. No Competition of RanGAP1 with RanGAP2 for Rx Binding, and PVX CP Does Not Interact with These RanGAPs.

ACKNOWLEDGMENTS

We are grateful to the Gatsby Charitable Foundation, the Biotechnology and Biological Sciences Research Council (BBSRC 83P/18617), and the European Union–funded Integrated Project Bioexploit (Contract FOOD-CT-2005-513959) for support. We thank colleagues Ericka Havecker, Carolina Casado, Frank Schwach, Nicolas Baumberger, and Manuel Montero for discussion, advice, and feedback and for providing materials;

Florian Kaffarnik and Alex Jones for mass spectrometry; and Matthew Smoker and Sharyn Carter for plant transformation. We thank Matthieu Joosten for critical reading of the manuscript and support and Peter Moffett and Jaap Bakker for providing information about unpublished results.

Received February 13, 2007; revised April 24, 2007; accepted May 3, 2007; published May 25, 2007.

REFERENCES

Ahlfors, R., Macioszek, V., Rudd, J., Brosche, M., Schlichting, R., Scheel, D., and Kangasjarvi, J. (2004). Stress hormone-independent activation and nuclear translocation of mitogen-activated protein kinases in *Arabidopsis thaliana* during ozone exposure. Plant J. **40:** 512–522.

Ausubel, F.M. (2005). Are innate immune signaling pathways in plants and animals conserved? Nat. Immunol. **6:** 973–979.

Azevedo, C., Betsuyaku, S., Peart, J., Takahashi, A., Noel, L., Sadanandom, A., Casais, C., Parker, J., and Shirasu, K. (2006). Role of SGT1 in resistance protein accumulation in plant immunity. EMBO J. **25:** 2007–2016.

Bendahmane, A., Farnham, G., Moffett, P., and Baulcombe, D.C. (2002). Constitutive gain-of-function mutants in a nucleotide binding site-leucine rich repeat protein encoded at the *Rx* locus of potato. Plant J. **32:** 195–204.

Bendahmane, A., Kanyuka, K., and Baulcombe, D.C. (1999). The *Rx* gene from potato controls separate virus resistance and cell death responses. Plant Cell **11:** 781–792.

Bendahmane, A., Kohn, B.A., Dedi, C., and Baulcombe, D.C. (1995). The coat protein of potato virus X is a strain-specific elicitor of *Rx1*-mediated virus resistance in potato. Plant J. **8:** 933–941.

Bendahmane, A., Querci, M., Kanyuka, K., and Baulcombe, D.C. (2000). *Agrobacterium* transient expression system as a tool for the isolation of disease resistance genes: Application to the *Rx2* locus in potato. Plant J. **21:** 73–81.

Blum, H., Beier, H., and Gross, H.J. (1987). Improved silver staining of plant proteins, RNA and DNA in polyacrylamide gels. Electrophoresis **8:** 93–99.

Burch-Smith, T.M., Schiff, M., Caplan, J.L., Tsao, J., Czymmek, K., and Dinesh-Kumar, S.P. (2007). A novel role for the TIR domain in association with pathogen-derived elicitors. PloS Biol. **5:** e38.

Cheong, Y.H., et al. (2003). BWMK1, a rice mitogen-activated protein kinase, locates in the nucleus and mediates pathogenesis-related gene expression by activation of a transcription factor. Plant Physiol. **132:** 1961–1972.

Deslandes, L., Olivier, J., Peeters, N., Feng, D.X., Khounlotham, M., Boucher, C., Somssich, I., Genin, S., and Marco, Y. (2003). Physical interaction between RRS1-R, a protein conferring resistance to bacterial wilt, and PopP2, a type III effector targeted to the plant nucleus. Proc. Natl. Acad. Sci. USA **100:** 8024–8029.

Deyoung, B.J., and Innes, R.W. (2006). Plant NBS-LRR proteins in pathogen sensing and host defense. Nat. Immunol. **7:** 1243–1249.

Dinesh-Kumar, S.P., Tham, W.H., and Baker, B.J. (2000). Structure-function analysis of the tobacco mosaic virus resistance gene *N*. Proc. Natl. Acad. Sci. USA **97:** 14789–14794.

Dong, X. (2004). NPR1, all things considered. Curr. Opin. Plant Biol. **7:** 547–552.

Farnham, G., and Baulcombe, D.C. (2006). Artificial evolution extends the spectrum of viruses that are targeted by a disease-resistance gene from potato. Proc. Natl. Acad. Sci. USA **103:** 18828–18833.

Feys, B.J., and Parker, J.E. (2000). Interplay of signaling pathways in plant disease resistance. Trends Genet. **16:** 449–455.

Jones, J.D., and Dangl, J.L. (2006). The plant immune system. Nature **444:** 323–329.

Kaminaka, H., Nake, C., Epple, P., Dittgen, J., Schutze, K., Chaban, C., Holt, B.F., Merkle, T., Schafer, E., Harter, K., and Dangl, J.L. (2006). bZIP10–LSD1 antagonism modulates basal defense and cell death in Arabidopsis following infection. EMBO J. **25:** 4400–4411.

Kohm, B.A., Goulden, M.G., Gilbert, J.E., Kavanagh, T.A., and Baulcombe, D.C. (1993). A potato virus X resistance gene mediates an induced, nonspecific resistance in protoplasts. Plant Cell **5:** 913–920.

Lam, E., Kato, N., and Lawton, M. (2001). Programmed cell death, mitochondria and the plant hypersensitive response. Nature **411:** 848–853.

Lee, J., Rudd, J.J., Macioszek, V.K., and Scheel, D. (2004). Dynamic changes in the localization of MAPK cascade components controlling pathogenesis-related (*PR*) gene expression during innate immunity in parsley. J. Biol. Chem. **279:** 22440–22448.

Leipe, D.D., Koonin, E.V., and Aravind, L. (2004). STAND, a class of P-loop NTPases including animal and plant regulators of programmed cell death: Multiple, complex domain architectures, unusual phyletic patterns, and evolution by horizontal gene transfer. J. Mol. Biol. **343:** 1–28.

Leister, R.T., Dahlbeck, D., Day, B., Li, Y., Chesnokova, O., and Staskawicz, B.J. (2005). Molecular genetic evidence for the role of *SGT1* in the intramolecular complementation of Bs2 protein activity in *Nicotiana benthamiana*. Plant Cell **17:** 1268–1278.

Ligterink, W., Kroj, T., zur Nieden, U., Hirt, H., and Scheel, D. (1997). Receptor-mediated activation of a MAP kinase in pathogen defense of plants. Science **276:** 2054–2057.

Liu, Y., Schiff, M., Marathe, R., and Dinesh-Kumar, S.P. (2002). Tobacco *Rar1*, *EDS1* and *NPR1/NIM1* like genes are required for *N*-mediated resistance to tobacco mosaic virus. Plant J. **30:** 415–429.

Lu, R., Malcuit, I., Moffett, P., Ruiz, M.T., Peart, J., Wu, A.J., Rathjen, J.P., Bendahmane, A., Day, L., and Baulcombe, D.C. (2003). High throughput virus-induced gene silencing implicates heat shock protein 90 in plant disease resistance. EMBO J. **22:** 5690–5699.

Martin, G.B., Brommonschenkel, S.H., Chunwongse, J., Frary, A., Ganal, M.W., Spivey, R., Wu, T., Earle, E.D., and Tanksley, S.D. (1993). Map-based cloning of a protein kinase gene conferring disease resistance in tomato. Science **262:** 1432–1436.

Meier, I. (2007). Composition of the plant nuclear envelope: Theme and variations. J. Exp. Bot. **58:** 27–34.

Merkle, T. (2001). Nuclear import and export of proteins in plants: A tool for the regulation of signalling. Planta **213:** 499–517.

Mestre, P., and Baulcombe, D.C. (2006). Elicitor-mediated oligomerization of the tobacco N disease resistance protein. Plant Cell **18:** 491–501.

Moffett, P., Farnham, G., Peart, J., and Baulcombe, D.C. (2002). Interaction between domains of a plant NBS-LRR protein in disease resistance-related cell death. EMBO J. **21:** 4511–4519.

Nurnberger, T., Brunner, F., Kemmerling, B., and Piater, L. (2004). Innate immunity in plants and animals: Striking similarities and obvious differences. Immunol. Rev. **198:** 249–266.

Palma, K., Zhang, Y., and Li, X. (2005). An importin alpha homolog, MOS6, plays an important role in plant innate immunity. Curr. Biol. **15:** 1129–1135.

Pan, Q., Wendel, J., and Fluhr, R. (2000). Divergent evolution of plant NBS-LRR resistance gene homologues in dicot and cereal genomes. J. Mol. Evol. **50:** 203–213.

Peart, J.R., Cook, G., Feys, B.J., Parker, J.E., and Baulcombe, D.C. (2002a). An *EDS1* orthologue is required for *N*-mediated resistance against tobacco mosaic virus. Plant J. **29:** 569–579.

Peart, J.R., et al. (2002b). Ubiquitin ligase-associated protein SGT1 is required for host and nonhost disease resistance in plants. Proc. Natl. Acad. Sci. USA **99:** 10865–10869.

Pedley, K.F., and Martin, G.B. (2005). Role of mitogen-activated protein kinases in plant immunity. Curr. Opin. Plant Biol. **8:** 541–547.

Rairdan, G.J., and Moffett, P. (2006). Distinct domains in the ARC region of the potato resistance protein Rx mediate LRR binding and inhibition of activation. Plant Cell **18:** 2082–2093.

Ratcliff, F., Martin-Hernandez, A.M., and Baulcombe, D.C. (2001). Tobacco rattle virus as a vector for analysis of gene function by silencing. Plant J. **25:** 237–245.

Ren, T., Qu, F., and Morris, T.J. (2005). The nuclear localization of the Arabidopsis transcription factor TIP is blocked by its interaction with the coat protein of *Turnip crinkle virus*. Virology **331:** 316–324.

Rose, A., and Meier, I. (2001). A domain unique to plant RanGAP is responsible for its targeting to the plant nuclear rim. Proc. Natl. Acad. Sci. USA **98:** 15377–15382.

Sacco, M., Mansoor, S., and Moffett, P. (2007). A RanGAP protein physically interacts with the NB-LRR protein Rx and is required for Rx-mediated viral resistance. Plant J., in press.

Salmeron, J.M., Oldroyd, G.E., Rommens, C.M., Scofield, S.R., Kim, H.S., Lavelle, D.T., Dahlbeck, D., and Staskawicz, B.J. (1996). Tomato *Prf* is a member of the leucine-rich repeat class of plant disease resistance genes and lies embedded within the *Pto* kinase gene cluster. Cell **86:** 123–133.

Schwach, F., Vaistij, F.E., Jones, L., and Baulcombe, D.C. (2005). An RNA-dependent RNA polymerase prevents meristem invasion by potato virus X and is required for the activity but not the production of a systemic silencing signal. Plant Physiol. **138:** 1842–1852.

Shen, Q.H., Saijo, Y., Mauch, S., Biskup, C., Bieri, S., Keller, B., Seki, H., Ulker, B., Somssich, I.E., and Schulze-Lefert, P. (2007). Nuclear activity of MLA immune receptors links isolate-specific and basal disease-resistance responses. Science **315:** 1098–1103.

Tai, T.H., Dahlbeck, D., Clark, E.T., Gajiwala, P., Pasion, R., Whalen, M.C., Stall, R.E., and Staskawicz, B.J. (1999). Expression of the *Bs2* pepper gene confers resistance to bacterial spot disease in tomato. Proc. Natl. Acad. Sci. USA **96:** 14153–14158.

Takken, F.L., Albrecht, M., and Tameling, W.I. (2006). Resistance proteins: Molecular switches of plant defence. Curr. Opin. Plant Biol. **9:** 383–390.

Tameling, W.I., Elzinga, S.D., Darmin, P.S., Vossen, J.H., Takken, F.L., Haring, M.A., and Cornelissen, B.J. (2002). The tomato *R* gene products I-2 and Mi-1 are functional ATP binding proteins with ATPase activity. Plant Cell **14:** 2929–2939.

Tameling, W.I., Vossen, J.H., Albrecht, M., Lengauer, T., Berden, J.A., Haring, M.A., Cornelissen, B.J., and Takken, F.L. (2006). Mutations in the NB-ARC domain of I-2 that impair ATP hydrolysis cause autoactivation. Plant Physiol. **140:** 1233–1245.

Tzfira, T., Vaidya, M., and Citovsky, V. (2001). VIP1, an Arabidopsis protein that interacts with *Agrobacterium* VirE2, is involved in VirE2 nuclear import and *Agrobacterium* infectivity. EMBO J. **20:** 3596–3607.

van der Krol, A.R., and Chua, N.H. (1991). The basic domain of plant B-ZIP proteins facilitates import of a reporter protein into plant nuclei. Plant Cell **3:** 667–675.

van der Vossen, E.A., van der Voort, J.N., Kanyuka, K., Bendahmane, A., Sandbrink, H., Baulcombe, D.C., Bakker, J., Stiekema, W.J., and Klein-Lankhorst, R.M. (2000). Homologues of a single resistance-gene cluster in potato confer resistance to distinct pathogens: A virus and a nematode. Plant J. **23:** 567–576.

Whitham, S., Dinesh-Kumar, S.P., Choi, D., Hehl, R., Corr, C., and Baker, B. (1994). The product of the tobacco mosaic virus resistance gene *N*: Similarity to Toll and the interleukin-1 receptor. Cell **78:** 1101–1115.

Zhang, Y., Dorey, S., Swiderski, M., and Jones, J.D. (2004). Expression of *RPS4* in tobacco induces an AvrRps4-independent HR that requires EDS1, SGT1 and HSP90. Plant J. **40:** 213–224.

Zhang, Y., Goritschnig, S., Dong, X., and Li, X. (2003). A gain-of-function mutation in a plant disease resistance gene leads to constitutive activation of downstream signal transduction pathways in *suppressor of npr1-1, constitutive 1*. Plant Cell **15:** 2636–2646.

Zhang, Y., and Li, X. (2005). A putative nucleoporin 96 is required for both basal defense and constitutive resistance responses mediated by *suppressor of npr1-1, constitutive 1*. Plant Cell **17:** 1306–1316.

Zipfel, C., and Felix, G. (2005). Plants and animals: A different taste for microbes? Curr. Opin. Plant Biol. **8:** 353–360.